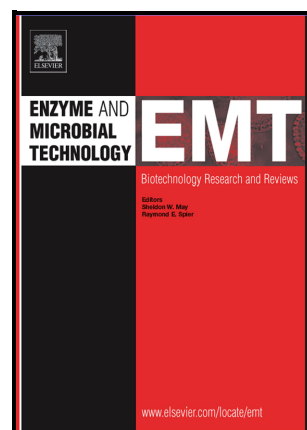


Application of Reductive Amination by Heterologously Expressed *Thermomicrobium roseum* L-alanine Dehydrogenase to Synthesize L-Alanine Derivatives

Huri Bulut, Jarkko Valjakka, Ossi Turunen, Berin Yilmazer, Ğarip Demir, Janne Jänis, Barış Binay



PII: S0141-0229(23)00073-X

DOI: <https://doi.org/10.1016/j.enzmictec.2023.110265>

Reference: EMT110265

To appear in: *Enzyme and Microbial Technology*

Received date: 8 February 2023

Revised date: 21 May 2023

Accepted date: 22 May 2023

Please cite this article as: Huri Bulut, Jarkko Valjakka, Ossi Turunen, Berin Yilmazer, Ğarip Demir, Janne Jänis and Barış Binay, Application of Reductive Amination by Heterologously Expressed *Thermomicrobium roseum* L-alanine Dehydrogenase to Synthesize L-Alanine Derivatives, *Enzyme and Microbial Technology*, (2023) doi:<https://doi.org/10.1016/j.enzmictec.2023.110265>

This is a PDF file of an article that has undergone enhancements after acceptance, such as the addition of a cover page and metadata, and formatting for readability, but it is not yet the definitive version of record. This version will undergo additional copyediting, typesetting and review before it is published in its final form, but we are providing this version to give early visibility of the article. Please note that, during the production process, errors may be discovered which could affect the content, and all legal disclaimers that apply to the journal pertain.

© 2023 Published by Elsevier.

Application of reductive amination by heterologously expressed *Thermomicrobium roseum* L-alanine dehydrogenase to synthesize L-alanine derivatives

Huri Bulut^a, Jarkko Valjakka^b, Ossi Turunen^c, Berin Yilmazer^d, Ğarip Demir^d, Janne Jänis^e, Barış Binay^{f, g*}

^a Medical Biochemistry Department, Faculty of Medicine, Istinye University, 34010, Istanbul, Turkey

^b Faculty of Medicine and Health Technology, Tampere University, FI-33100 Tampere, Finland

^c School of Forest Sciences, University of Eastern Finland, FI-80101 Joensuu, Finland

^d Department of Molecular Biology and Genetics, Gebze Technical University, 41400, Gebze, Kocaeli, Turkey

^e Department of Chemistry, University of Eastern Finland, FI-80101 Joensuu, Finland

^f Department of Bioengineering, Gebze Technical University, 41400, Gebze, Kocaeli, Turkey

^g BAUZYME Biotechnology Co., Gebze Technical University Technopark, 41400, Gebze, Kocaeli, Turkey

*Corresponding Author Details:

Baris Binay, Assoc. Prof. Dr., (ORCID ID: 0000-0002-6190-6549)

Department of Bioengineering, Gebze Technical University,

41400, Gebze, Kocaeli, Turkey

+90 262 605 2080

binay@gtu.edu.tr

ABSTRACT

Unnatural amino acids are unique building blocks in modern medicinal chemistry as they contain an amino and a carboxylic acid functional group, and a variable side chain. Synthesis of pure unnatural amino acids can be made through chemical modification of natural amino acids or by employing enzymes that can lead to novel molecules used in the manufacture of various pharmaceuticals. The NAD⁺-dependent alanine dehydrogenase (AlaDH) enzyme catalyzes the conversion of pyruvate to L-alanine by transferring ammonium in a reversible reductive amination activity. Although AlaDH enzymes have been widely studied in terms of oxidative deamination activity, reductive amination activity studies have been limited to the use of pyruvate as a substrate. The reductive amination potential of heterologously expressed, highly pure *Thermomicrobium roseum* alanine dehydrogenase (TrAlaDH) was examined with

regard to pyruvate, α -ketobutyrate, α -ketovalerate and α -ketocaproate. The biochemical properties were studied, which included the effects of 11 metal ions on enzymatic activity for both reactions. The enzyme accepted both derivatives of L-alanine (in oxidative deamination) and pyruvate (in reductive amination) as substrates. While the kinetic K_M values associated with the pyruvate derivatives were similar to pyruvate values, the kinetic k_{cat} values were significantly affected by the side chain increase. In contrast, K_M values associated with the derivatives of L-alanine (L- α -aminobutyrate, L-norvaline, and L-norleucine) were approximately two orders of magnitude greater, which would indicate that they bind very poorly in a reactive way to the active site. The modeled enzyme structure revealed differences in the molecular orientation between L-alanine/pyruvate and L-norleucine/ α -ketocaproate. The reductive activity observed would indicate that TrAlaDH has potential for the synthesis of pharmaceutically relevant amino acids.

Keywords: unnatural amino acids, medicinal chemistry, Alanine dehydrogenase, *Thermomicrobium roseum*, reductive amination mechanism, α -keto acids, molecular modeling

Introduction

Unnatural amino acids (UAA) play an important role in the production of pharmaceuticals, with an increasingly large pool used as modular building blocks in drug development, broadening their future applications [1]. However, the latter strictly depends on UAA being synthesized at a high purity-enantiopure level prior to the drug formulation process proceedings [2,3]. Enzymatic methods are widely preferred for cost-effective asymmetric synthesis of UAA. Asymmetric synthesis of L-alanine (L-Ala) derivatives (as the smallest member of the unnatural amino acid family) is invaluable since the derivatives are the basic units for structural modification and novel molecules for medicinal chemistry. In particular, enzymatic reductive amination reaction of NAD^+ - dependent alanine

dehydrogenase (AlaDH) has shown considerable potential for asymmetric synthesis of L-Ala derivatives [4-7]. In microorganisms, AlaDH assists in redox balancing as its deamination/amination reaction is linked to the reduction/oxidation of NAD^+/NADH . Moreover, AlaDH [L-alanine: nicotinamide adenine dinucleotide (NAD)⁺-oxidoreductase (deaminating) EC 1.4.1.1] is a catalyst for the oxidizing deamination of L-Ala and the reductive amination of oxyacid (**Figure 1**).

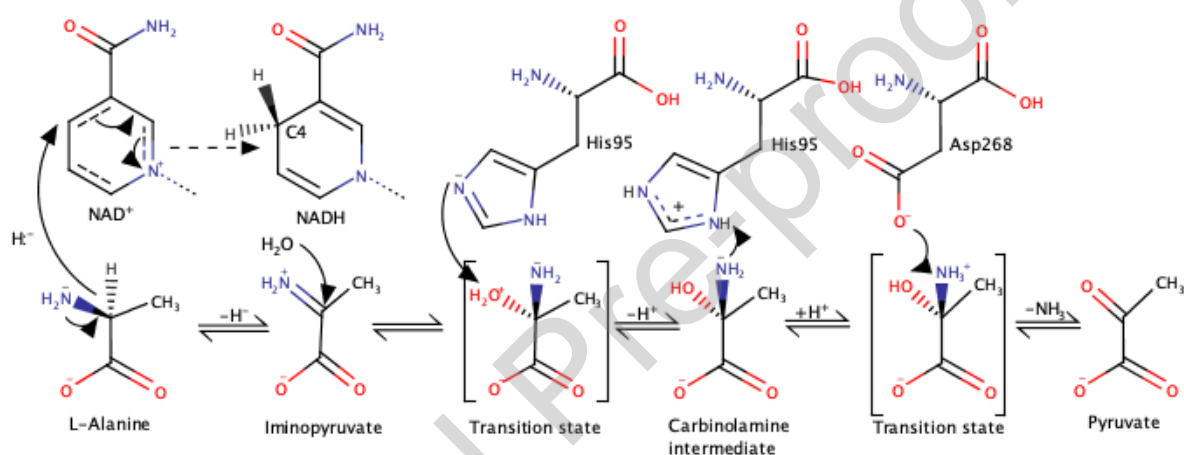


Fig. 1 Reaction mechanism for oxidative deamination and reductive amination by *Thermomicrobium roseum* alanine dehydrogenase (*TrAlaDH*). Numbering is according to the *TrAlaDH* sequence.

Numerous L-AlaDH enzymes, mainly from mesophilic organisms, have been identified via purification, and partial kinetic and biochemical characterizations have been performed, although most studies were limited to the analysis of oxidative deamination activity [6,8-19]. To date, AlaDH reductive amination activity studies have been limited to the use of pyruvate [19-22], while a biochemical and computational study that proposes an AlaDH reductive amination activity mechanism model for α -keto acid derivatives of pyruvate has not yet been reported.

The present study investigates, for the first time, a comparative biochemical, computational study of the potential of *Thermomicrobium roseum* alanine dehydrogenase

(*TrAlaDH*) for reductive amination activity with α -ketobutyrate, α -ketovalerate and α -ketocaproate as pyruvate derivatives. This can be more efficient to synthesize their matching L-alanine derivatives as unnatural amino acids. A computationally developed paradigm for the *TrAlaDH* catalytic reductive amination mechanism model was also studied in respect to the observed biochemical-kinetic oxidative deamination activity against L-alanine and selected derivatives L- α -aminobutyrate, L-norvaline, and L-norleucine.

Materials and Methods

Microorganism, chemicals, and kits

All chemicals were purchased from Sigma-Aldrich (St. Louis, MO, USA) and Thermo Fisher (Waltham, MA, USA). Transformation competent *Escherichia coli* DH-5 α and BL21 (DE3) cells were purchased from New England Biolabs (Ipswich, MA, USA) and Invitrogen (Waltham, MA, USA). Plasmid purification kits were purchased from Invitrogen, and BCA Protein Assay kits were purchased from Thermo Fisher Scientific. All culture media were prepared from chemicals purchased from LABM (Bury, UK), and PageRuler™ Plus Prestained Protein Ladder was purchased from Thermo Fisher Scientific. Anti-His-tag and horseradish peroxidase (HRP) were used as primary and secondary antibodies, respectively, and were purchased from Abcam (Cambridge, UK). Western Blotting Luminol Reagent was purchased from Santa Cruz, TX, USA, an Ni-NTA HisTrap column was purchased from General Electric (Boston, MA, USA), and filters and PD-10 columns were purchased from MilliporeSigma (Burlington, MA, USA).

Cloning of the *T. roseum ald* gene into pET28a (+) vector

The *ald* gene (UniProt accession number: B9L0I6) from *T. roseum* (ATCC 27502 / DSM 5159 / P-2) coding for AlaDH enzyme was optimized by codon usage preference for *E.*

coli expression. The codon optimized gene was purchased from GeneUniversal (Newark, USA). The synthesized gene of TrAlaDH was ligated into the pET-28a+ plasmid and transformed into NEB[®] 5-alpha competent *E. coli* cells. The recombinant plasmid pET28a+ contains the complete alanine dehydrogenase coding region with NdeI/XhoI restriction sites and the 6xHis-tag at the N-terminal end.

Expression and purification of TrAlaDH

E. coli BL21 (DE3) cells were used as the host to express *traladh* in the pET-28a+ plasmid. *E. coli* BL21 (DE3) cells with recombinant pET28a+ were plated on LB-agar (Luria–Bertani) that contained kanamycin (50 µg/ml). Cultivation was scaled up to a 500 mL culture, which was incubated at 37 °C at 200 x g. Studier autoinduction media (at 30 °C for 16 hours) was used for induction [23]. The pellets were harvested via centrifugation at 8000 x g for 20 min at 4 °C.

For purification, the cell pellets were resuspended in lysis buffer (50 mM phosphate buffer, pH 8.0, 300 mM NaCl and 1 mM phenylmethylsulfonyl fluoride [PMSF]), and cell suspensions were sonicated on ice with a Soniprep 150 sonicator (Sanyo, Tokyo, Japan). The cell lysates were centrifuged, and the obtained supernatants were filtered with a 0.45 µm filter (Millipore Co, USA). Then, the filtrates were loaded onto the Ni-NTA HisTrap column (General Electric, USA), regenerated and equilibrated with Buffer A (20 mM NaH₂PO₄, 30 mM NaCl, 30 mM imidazole, pH 7.4) and Buffer B (20 mM NaH₂PO₄, 30 mM NaCl, 500 mM imidazole, pH 7.4). Column chromatography was performed using the ÄKTA pure system (GE Healthcare, USA) at 4 °C using Buffer A and B with different imidazole concentrations (100–400 mM). After purification, the collected samples were analyzed on 12% SDS–PAGE performed on the Miniprotean II electrophoresis cell system (Bio-Rad, USA) with Coomassie brilliant blue R-250 to identify the fractions that contain pure protein

bands. Proteins were concentrated with ultracentrifuge tubes, and a PD-10 column (Millipore, USA) was used for further purification. Protein concentration was measured with the Bradford Assay Kit (Thermo Fisher Scientific, USA) and bovine serum albumin (BSA) was used as a standard.

The presence of the recombinant *TrAlaDH* protein was also confirmed by Western Blot analysis (Western Blot system, Biorad, USA) using an anti-6xHis Tag antibody and a horseradish peroxidase secondary antibody.

Biochemical characterization of pH, temperature and the effects of metal ions on enzymatic activity

Optimum pH levels for oxidative deamination and reductive amination were assayed with the following buffers, which cover the pH range from 5 to 12: 100 mM sodium phosphate for pH 5 and 6, 100 mM Tris-HCl for pH 7–9, 100 mM glycine NaOH for pH 10, and 100 mM sodium bicarbonate for pH 11 and 12. The reactions were performed in a 96-well microplate at 300 μ L volumes. The reaction mixture for the oxidative deamination was L-alanine (25 mM), NAD^+ (1.4 mM) and enzyme in the optimized buffer. The reaction mixture for the reductive amination was NH_4Cl (2 M), pyruvate (4.5 mM), NADH (0.27 mM) and the enzyme (0.5 mg/mL) in the optimized buffer.

To evaluate the effect of temperature on enzymatic oxidative deamination and reductive amination activity, measurements were performed at different temperatures (20–80 $^{\circ}\text{C}$).

The effects of 6 different concentrations of 11 metal ions on enzymatic oxidative deamination and reductive amination activity were investigated: chloride salts of Cu(II), Fe(III), Ca(II), Li(I), Mg(II), Mn(II), K(I), Na(I), Zn(II), metallic tungsten (W) as powder, and Mo(VI) as sodium salt were added to the reaction mixture to obtain different final

concentrations (1, 3, 5, 7, 10, 100 μM), respectively. All reaction absorbances were measured in triplicate by a microplate reader (Varioscan, Thermo Fisher Scientific, USA) at 340 nm at 10 sec intervals for 10 min at 25 °C.

Kinetic Assays

The oxidative deamination and reductive amination activities of *TrAlaDH* with regard to L-alanine/L- α -aminobutyrate/L-norvaline/L-norleucine/pyruvate/ α -ketobutyrate/ α -ketovalerate/ α -ketocaproate were assayed under the determined optimum reaction conditions by noting the change in the amount of NAD(H) at 340 nm in the microplate reader [24]. The reaction mixture for oxidative deamination and reductive amination within a specified range of L-alanine concentrations was (1–5 mM)/L- α -aminobutyrate (100–700 mM)/L-norvaline (100–700 mM)/L-norleucine (100–700 mM) with NAD^+ (1.4 mM; 0.153–15 mM) and a range of α -keto derivatives (α -ketobutyrate/ α -ketovalerate/ α -ketocaproate); 0.1–15 mM) with pyruvate (1–10 mM), NH_4Cl (2 M; 0.25–3 M), NADH (0.27 mM; 0.5–5 mM) and the enzyme (0.5 mg/mL) in the optimized buffer. Control groups contained the enzyme in the optimized buffer and NAD(H) for the oxidative deamination and reductive amination.

The kinetic parameters (K_M , k_{cat}) were calculated for selected substrates and coenzyme concentrations by fitting data to Michaelis-Menten plots with GraphPad Prism 8.0 (GraphPad Software, San Diego, USA) using nonlinear least-squares regression. One unit described the amount of enzyme that transformed 1 μmol of substrate per minute to the product. Reaction mixtures for oxidative deamination or reductive amination included a range of substrates at different concentration with specified NAD^+ or NADH and enzyme in the optimum pH buffer [22]. Furthermore, the conversion efficiency of *TrAlaDH* on selected substrates was calculated by consumption of NADH per time [25].

Molecular modeling

The 3-dimensional structure of *TrAlaDH* was modeled with the Swiss-Model [26] using the crystal structure of *Mycobacterium tuberculosis* AlaDH (2voj.pdb: 50.95% sequence identity) as a template [27]. 2voj.pdb structure contains both the NAD⁺ cofactor and pyruvate at the active site. Residues of Arg15, Lys74, Tyr93, His95, Leu128, Met131, Ile267, Asp268, Gln269, Gly270, Asn299, and Pro301 in the active site are fully conserved between the template and *TrAlaDH* and also in larger AlaDH enzyme group (alignment in supplementary material, **Figure S1**). L-alanine, L-norleucine and α -ketocaproate were manually transferred in Swiss-PdbViewer to superimpose pyruvate in 2voj structure. After this, energy minimization calculations were performed using the YASARA energy minimization server [28]. Then, comparison of the structures was performed, and images drawn, using the Chimera program (**Figure 6**) [29]. To describe the enzymatic catalysis, the minimization energy for the complex structures formed by the L-alanine and L-norleucine and substrates and the pyruvate and α -ketocaproate products were calculated in the presence of explicit water molecules. Thus, observable changes in the binding interactions were comparable.

Results

Cloning, expression, and purification of *TrAlaDH*

Overexpression of *TrAlaDH* was accomplished using *E. coli* BL21 (DE3) as the host cell. The cell cultures were incubated for 16 h at 30 °C in an auto-induction Studier medium for protein expression. The expressed protein was purified using an affinity chromatography column, and the collected samples were analyzed on SDS-PAGE (**Figure 2**). Purified enzyme was 2.5 mg/mL. The presence of *TrAlaDH* was confirmed using Western blot analysis (**Figure 3**). A single major protein band in both SDS-PAGE and Western blot indicated that

TrAlaDH had been successfully expressed in *E. coli*. The molecular mass of the highly purified enzyme was 42 kDa.

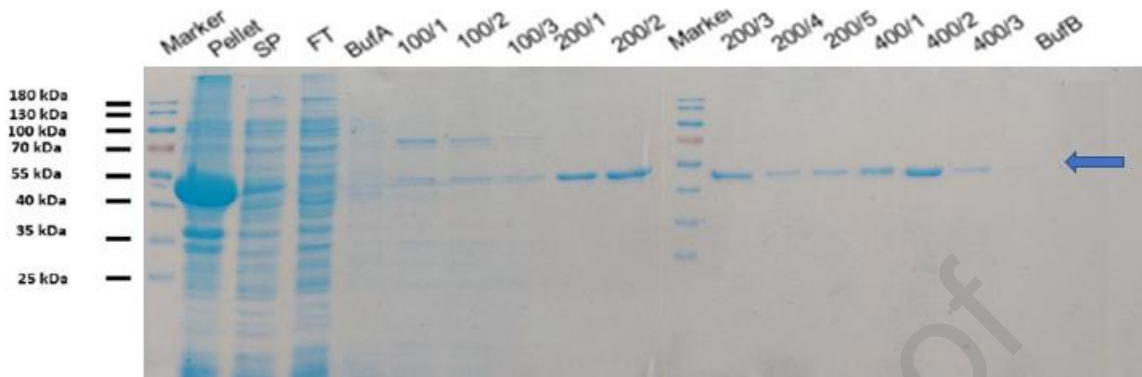


Fig. 2 SDS-PAGE gel analysis after *Thermomicrobium roseum* alanine dehydrogenase (*TrAlaDH*) purification (Marker, Pellet, Supernatant, FT: column passed sample, Buffer A (BufA) 100-200-400 mM, Buffer B (BufB) elution fractions). Buffer A consisted of 20 mM NaPi, 500 mM NaCl, and 30 mM imidazole at pH 7.4, while Buffer B contained 20 mM NaPi, 500 mM NaCl, and 500 mM imidazole at pH 7.4. Each buffer was prepared with varying concentrations of imidazole, namely 100 mM, 200 mM, and 400 mM. These buffers were utilized to facilitate the separation and purification of the target substance. By applying an imidazole gradient, the target proteins were separated and obtained as fractions from the column. The fractions collected after washing the purification column were designated as Buffer A, with the numbers 1, 2, and 3 indicating the respective fractions. For example, 100/1 referred to Fraction 1 containing 100 mM imidazole. Buffer B indicated the passage of a solution containing 500 mM imidazole through the column.

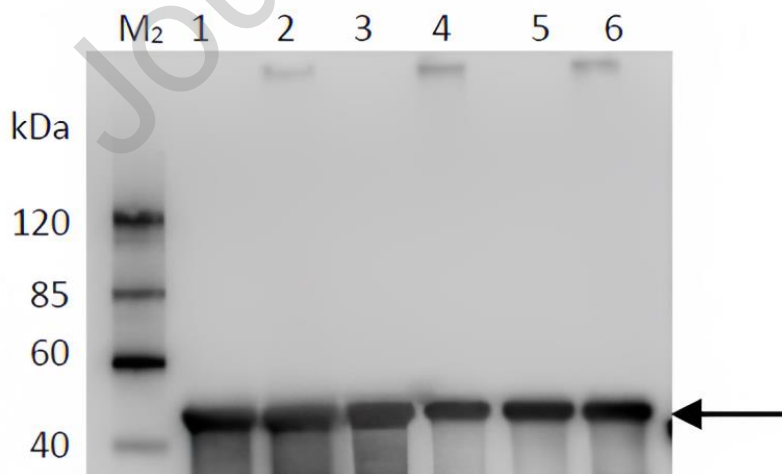


Fig. 3 Western blot analysis of *Thermomicrobium roseum* alanine dehydrogenase (*TrAlaDH*) protein expression. Lanes: M, Molecular weight marker; 1: cell lysate; 2–6: fractions eluted with 200 mM imidazole.

Biochemical properties of the recombinant *TrAlaDH*

We investigated the effects of pH and temperature on *TrAlaDH* by monitoring the change in enzymatic activity within a pH range 5–12 and a temperature range 25–80 °C. Thermostability of the enzyme was also determined. The pH activity profile showed that the enzyme was highly active at pH 8–10 for both oxidative deamination (**Figure 4a**) and reductive amination (**Figure 4b**).

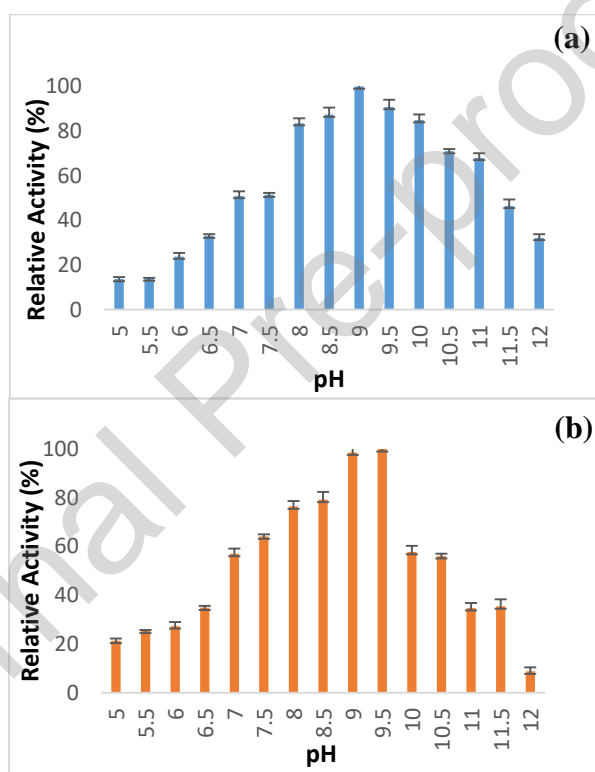


Fig. 4 Dependence of *Thermomicrobium roseum* alanine dehydrogenase (*TrAlaDH*) activity on pH levels. **(a)** Effect of pH on oxidative deamination reactions, and **(b)** effect on reductive amination reactions. The experiments were carried out at 25 °C.

The greatest activity levels were observed at pH 9 for oxidative deamination and at pH 9.5 for reductive amination, both at 25 °C. The enzyme was found to maintain its activity in both directions under neutral and basic conditions. The effect of temperature on oxidative deamination and reductive amination activity in *TrAlaDH* was investigated by monitoring the

change in enzymatic activity in the temperature range 25–80 °C. The enzyme exhibited greatest oxidative deamination (**Figure 5a**) and reductive amination activity (**Figure 5b**) at approximately 55 °C.

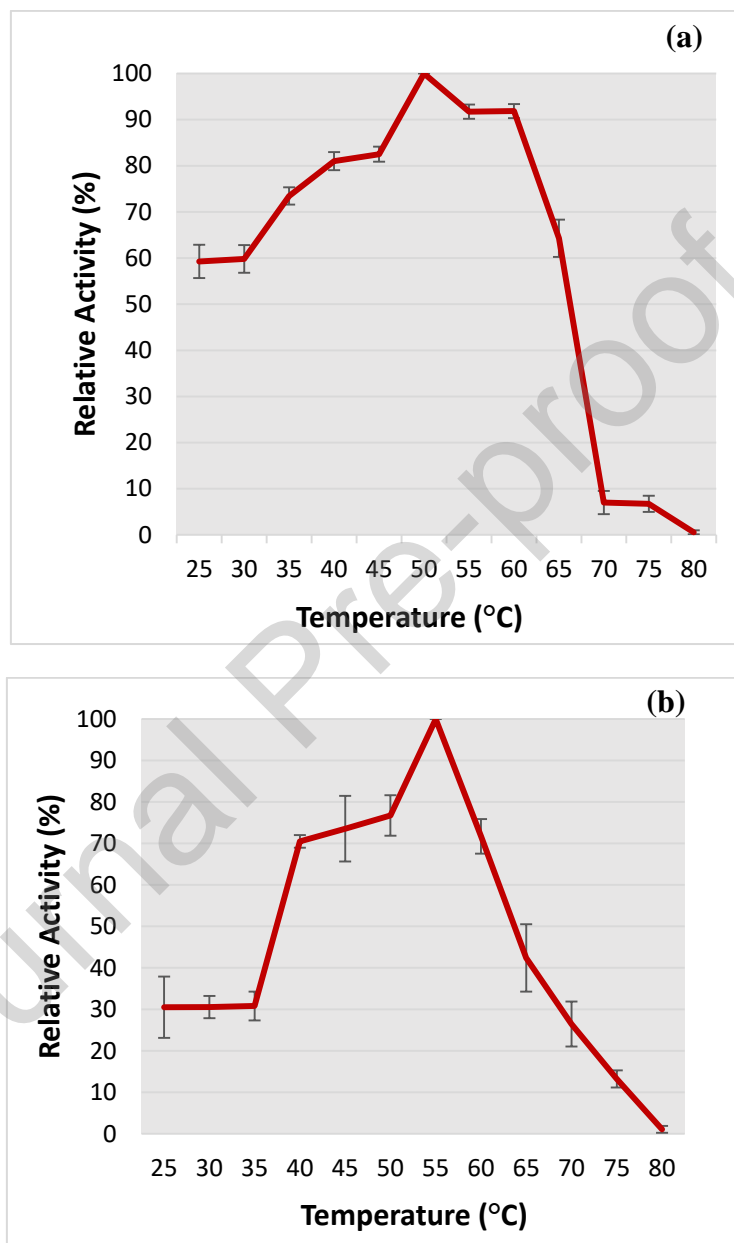
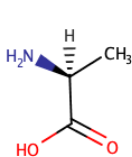
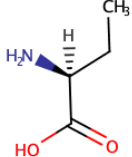
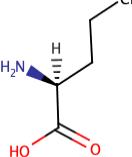
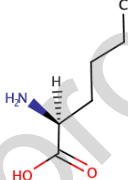
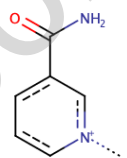
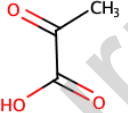
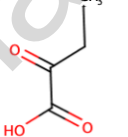
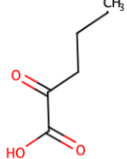
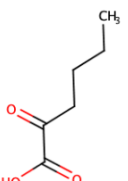
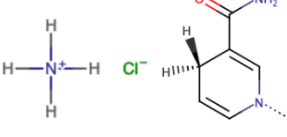


Fig. 5. Dependence of *Thermomicrobium roseum* alanine dehydrogenase (TrAlaDH) activity on temperature. (a) Temperature effect on oxidative deamination reactions, and (b) effect on reductive amination reactions. The oxidative deamination was performed at pH 9 and reductive amination at pH 9.5.

The kinetic parameters of *TrAlaDH* were determined for both oxidative deamination and reductive amination reactions by fitting data to Michaelis-Menten plots (in supplementary material, **Figure S2**) (**Table 1**).

Table 1. Kinetic parameters for *Thermomicrobium roseum* alanine dehydrogenase (*TrAlaDH*) with L-alanine and derivatives in oxidative deamination and reductive amination reactions. Molecular structures are also shown for L-alanine and derivatives.

| Oxidative Deamination | | | | | | |
|--|---|---|---|--|---|-----------------|
| |  |  |  |  |  | |
| | L-Alanine | L- α -aminobutyrate | L-Norvaline | L-Norleucine | NAD ⁺ | |
| K_M (mM) | 3.21 \pm 0.3 | 248.1 \pm 0.3 | 179.1 \pm 0.40 | 353.7 \pm 0.70 | 3.0 \pm 0.20 | |
| k_{cat} (s ⁻¹) | 4.73 \pm 0.1 | 23.30 \pm 0.2 | 0.25 \pm 0.30 | 0.40 \pm 0.40 | 3.90 \pm 0.20 | |
| k_{cat}/K_M (M ⁻¹ s ⁻¹) | 1.47 \pm 0.2 | 0.094 \pm 0.1 | 0.0014 \pm 0.01 | 0.0011 \pm 0.20 | 1.30 \pm 0.20 | |
| Reductive Amination | | | | | | |
| |  |  |  |  |  | |
| | Pyruvate | α -ketobutyrate | α -ketovalerate | α -ketocaproate | NH ₄ Cl | NADH |
| K_M (mM) | 1.90 \pm 0.20 | 1.30 \pm 0.2 | 1.70 \pm 0.20 | ND* | 4.30 \pm 0.50 | 3.60 \pm 0.50 |
| k_{cat} (s ⁻¹) | 35.0 \pm 0.50 | 1.50 \pm 0.2 | 1.29 \pm 0.10 | ND* | 2.40 \pm 0.30 | 7.10 \pm 0.20 |
| k_{cat}/K_M (M ⁻¹ s ⁻¹) | 18.40 \pm 0.10 | 1.20 \pm 0.3 | 0.76 \pm 0.20 | ND* | 0.50 \pm 0.20 | 2.0 \pm 0.10 |

ND*: Non defined

The measured Michaelis-Menten constant values (range 1.3–1.9 mM) showed a clear affinity for enzyme binding for pyruvate, α -ketobutyrate and α -ketovalerate. In oxidative deamination, the K_M values (excluding L-alanine) were considerably greater, which indicates significant problems in binding in a reactive way onto the active site. In both reactions, the turnover rate k_{cat} values dropped considerably with the larger substrates, with the exception of L- α -aminobutyrate. Due to changes in the K_M and k_{cat} values, the calculated catalytic

efficiency values k_{cat}/K_M also dropped considerably for all derivatives when compared to L-alanine or pyruvate, respectively. There was a 1363-fold decrease in the k_{cat}/K_M value associated with L-norleucine. Only α -ketocaproate could not be measured.

Conversion efficiency of *TrAlaDH* is shown in **Table 2**. Conversions is expressed in percentage change per min as calculated from NADH consumption. *TrAlaDH* enzyme reached 54% conversion of pyruvate in the used substrate concentration per min, whereas only 15% conversion rate was observed for L-alanine. The conversion rates are quite high also for L- α -aminobutyrate α -ketobutyrate α -ketovalerate. These values show that the enzyme functions quite efficiently with several substrates. On the other hand, conversion rate could not be determined for α -ketocaproate.

Table 2. Conversion efficiency of *TrAlaDH* on different substrates

| Substrates | Conversion (%) min^{-1} |
|----------------------------|-------------------------------------|
| L-alanine | 15 |
| L- α -aminobutyrate | 28 |
| L-norvaline | 7 |
| L-norleucine | 5 |
| Pyruvate | 54 |
| α -ketobutyrate | 22 |
| α -ketovalerate | 21 |
| α -ketocaproate | ND* |

ND*: Non defined

Effect of metal ions on *TrAlaDH* activity

The effects of group 2A elements on the dehydrogenase family are available in the literature [30, 31]. The effects of 11 metal ions on *TrAlaDH* activity were investigated for both oxidative deamination and reductive amination reactions. A standard enzyme assay was performed in the presence of six different concentrations of metal ions (**Table 3**).

Table 3. Effect of metal ions on the oxidative deamination and reductive amination reactions of *Thermomicrobium roseum* alanine dehydrogenase (*TrAlaDH*). Effects are shown with heatmap colors, which indicate a change in the activity of the *TrAlaDH* enzyme relative to the control (no metal ion addition). Green indicates greater activity in the presence of a metal ion and red indicates lower activity. The ANOVA test showed statistically significant values. The white and italic values indicate a change in the statistical significance, $p < 0.05$. The underlined values are statistically almost significant, $p < 0.01$.

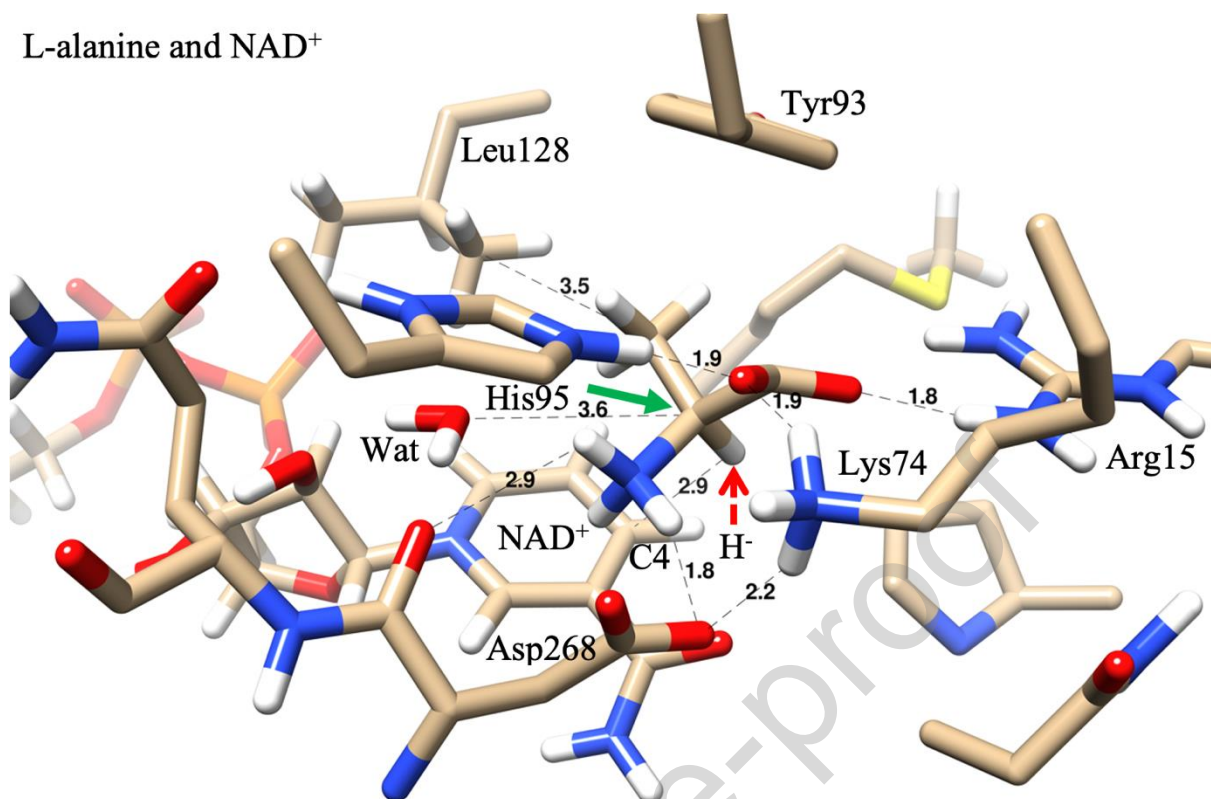
| Metals | Relative Activity (%) of oxidative deamination | | | | | | Relative Activity (%) of reductive amination | | | | | |
|------------------|--|---------------|---------------|----------------|---------------|---------------|--|-----------|----------------|----------------|---------------|---------------|
| | 1 μ M | 3 μ M | 5 μ M | 7 μ M | 10 μ M | 100 μ M | 1 μ M | 3 μ M | 5 μ M | 7 μ M | 10 μ M | 100 μ M |
| Control | 100 | 100 | 100 | 100 | 100 | 100 | 100 | 100 | 100 | 100 | 100 | 100 |
| Li ⁺ | 100±2.1 | 102±2.6 | 103±2.4 | 104±2.9 | 104±2.5 | 106±4.7 | 100±4.7 | 103±3.7 | <u>108±2.7</u> | 105±3.9 | 103±3.3 | 99±6.7 |
| Na ⁺ | 100±4.5 | 98±3.5 | 95±2.5 | <i>90±2.7</i> | <i>88±3.1</i> | <i>86±6.5</i> | 99±3.2 | 103±3.9 | 105±3.7 | 108±2.4 | 106±2.0 | 102±4.1 |
| K ⁺ | <i>99±2.4</i> | <i>96±1.1</i> | <i>94±1.6</i> | <i>92±1.6</i> | <i>85±2.7</i> | <i>83±1.8</i> | 100±1.7 | 102±1.5 | 105±1.3 | <u>110±2.3</u> | 103±4.4 | 98±2.3 |
| Mg ²⁺ | 100±2.0 | 99±2.6 | 98±2.5 | 92±2.2 | 90±2.7 | 88±4.7 | 99±2.4 | 98±3.1 | 99±3.6 | <i>90±2.3</i> | <i>89±4.4</i> | <i>90±3.6</i> |
| Ca ²⁺ | 98±4.1 | 96±1.3 | 98±0.9 | 96±2.4 | 95±1.7 | 95±2.2 | 99±2.5 | 98±2.3 | 98±3.1 | 99±3.1 | 97±2.8 | 95±3.9 |
| Mn ²⁺ | 100±0.5 | 100±1.3 | 103±1.0 | 104±2.1 | 105±4.2 | 105±2.1 | 99±2.6 | 100±1.3 | 102±1.8 | 105±1.8 | 102±2.9 | 99±2.1 |
| Cu ²⁺ | 96±3.5 | 95±0.7 | 96±2.0 | 98±1.5 | 92±3.3 | 90±0.9 | 96±4.5 | 95±1.8 | 96±1.4 | 98±2.8 | 92±2.2 | 90±2.6 |
| Zn ²⁺ | 100±2.2 | 97±2.9 | 95±3.4 | 92±2.1 | 90±4.2 | <i>81±5.4</i> | 99±2.3 | 96±2.8 | 97±2.7 | 93±3.2 | 89±2.7 | <i>84±4.9</i> |
| Fe ³⁺ | <i>93±2.3</i> | <i>92±2.1</i> | <i>90±2.9</i> | <i>89±2.9</i> | <i>85±2.6</i> | <i>78±3.7</i> | 94±3.7 | 90±0.9 | 89±2.2 | 88±1.7 | 82±3.5 | 80±1.2 |
| Mo ⁶⁺ | 99±1.9 | 100±3.6 | 98±1.1 | 97±1.9 | 95±2.6 | 92±6.7 | 100±2.2 | 98±3.8 | 99±1.4 | 95±2.2 | 94±2.8 | 95±6.9 |
| W ⁶⁺ | 102±2.9 | 103±3.7 | 104±3.7 | <u>108±2.2</u> | 111±1.8 | 111±3.8 | 99±2.2 | 100±2.8 | 101±2.7 | 102±2.3 | 105±2.9 | 102±5.1 |

We found that 100 μ M Fe³⁺ resulted in the greatest inhibition of the deamination reaction (~20% inhibition), with 100 μ M Zn²⁺ second (Table 3). At greater concentrations, tungsten (W⁶⁺) had an increasing effect on oxidative reactions, but less so on reductive reactions (maximum 11% activation). In addition, Na⁺ and K⁺ showed clear inhibition of deamination but no inhibition of amination was observed. However, the effect of the metals was minimal, even at 100 μ M concentrations.

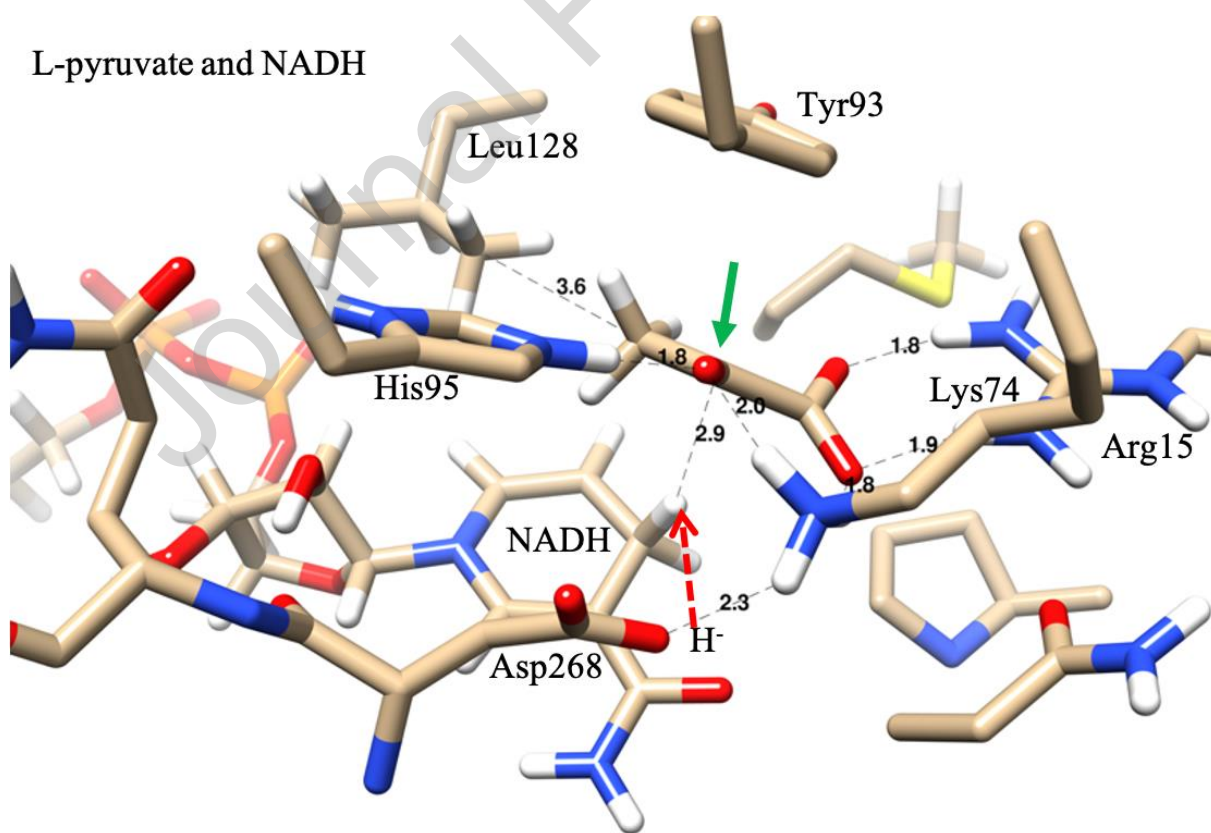
TrAlaDH enzyme and its active site modeling

The reversible catalytic mechanism [45] for oxidative deamination and reductive amination for *TrAlaDH* is described in Figure 1. It shows the active amino acids, which are involved in the transfer of electrons between the acceptor and the donor. The structures for the active molecules of the forward and reverse reactions at their first and final positions have

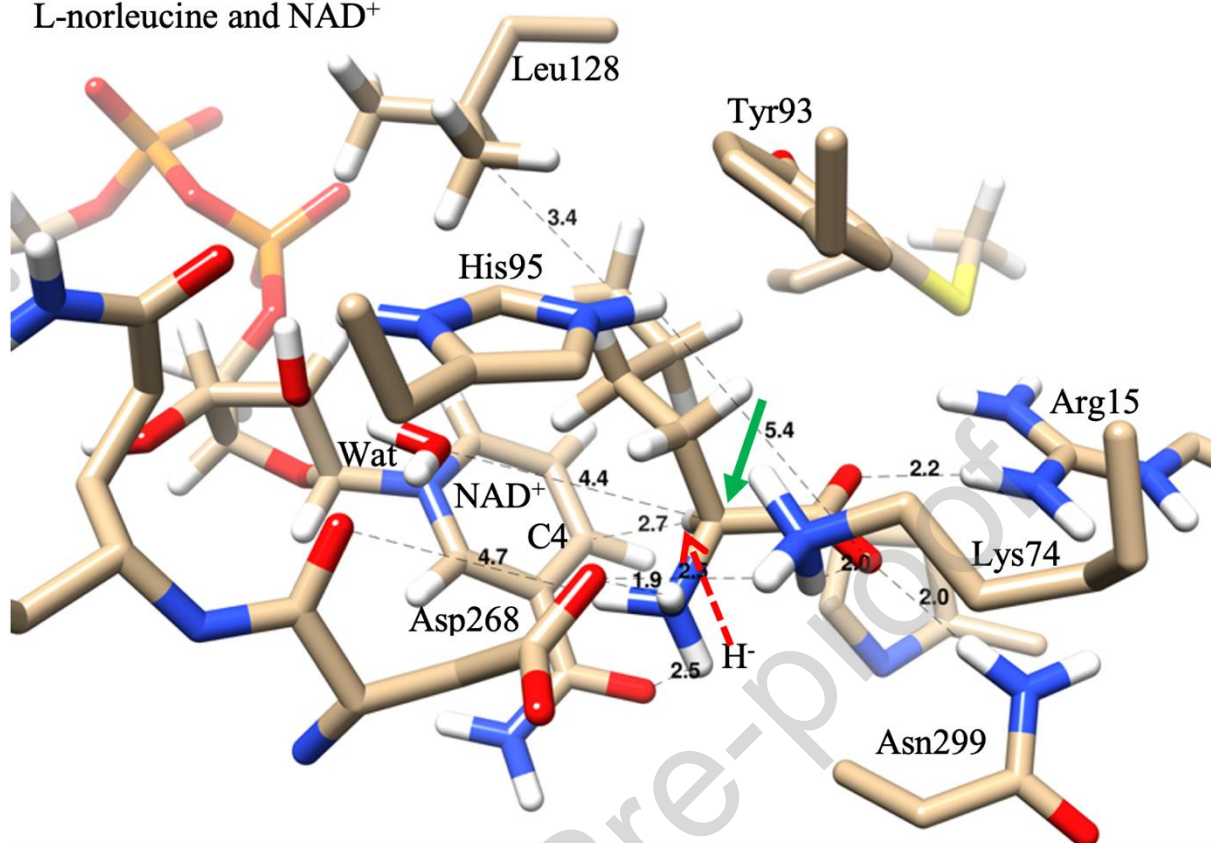
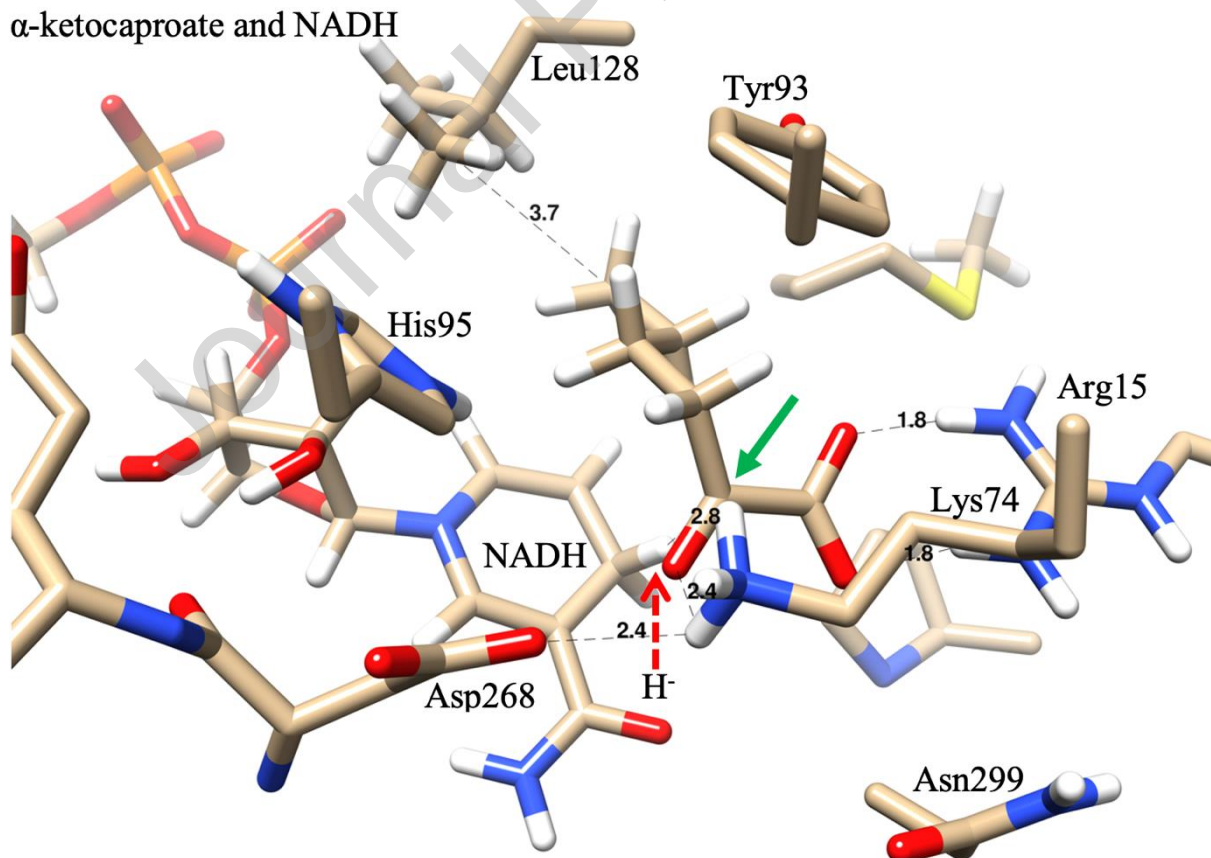
been modelled using the YASARA energy minimization server [28]. Description of the TrAlaDH reaction mechanism is consistent with the structures of the earlier publications [27,54]. There are some detectable differences in the binding interaction between L-alanine and L-norleucine at the active site before the reaction transition state is reached. The observed differences in reaction kinetics can be principally explained by the hydrogen bonds of the -NH₃ and -COO⁻ groups; during binding, their spatial orientation differs (**Figure 6**). The carboxylate group of alanine binds with hydrogen bonds Arg15, Lys74 and His95. The hydrogen bonds of the Asp268 side chain and its main oxygen chain are also involved in the orientation. In the case of L-norleucine, there are less hydrogen bonds at the active site, and they are formed with Arg15, His95 and Asp299. The hydrophobic residue Leu128 has clear contact with the methyl groups of L-alanine and L-norleucine. The distances between the leaving hydrides of C_α of L-alanine and L-norleucine and the reactive C4 of the NAD⁺ are 2.9 and 2.7 Å, respectively. The Asp268 carbonyl group in the P-loop of the NAD-binding Rossman fold appears to interact with the substrate. The P-loop may also be involved in the orientation of the water molecule, which is needed for the reaction. In the case of C_α of L-alanine and L-norleucine, the water distance is 3.6 and 4.4 Å, respectively (**Figure 6**).

L-alanine and NAD⁺

L-pyruvate and NADH



(a)

L-norleucine and NAD⁺ α -ketocaproate and NADH

(b)

Fig. 6 (a) The oxidative deamination reaction of *Thermomicrobium roseum* alanine dehydrogenase (*TrAlaDH*) with L-alanine to pyruvate. Oxygen is shown in red, nitrogen in blue, carbon in light brown and protons in white. The active site structures before and after the transition state are shown for key reaction stages for the hydride shift (hydride shown with red arrow) from L-alanine to NAD^+ , and the transfer of a water molecule to form pyruvate (Wat). The interaction distances between the L-alanine substrate and the pyruvate product are shown in Ångströms. In the upper part of the graphic, the L-alanine substrate (C_α shown with green arrow) is bound to three hydrogen bonds formed by the carboxylate group ($-\text{COO}^-$): to Arg15 (1.8 Å), Lys74 (1.9 Å) and His95 (1.9 Å). In addition, its amino group ($-\text{CH}_3^+$) binds with two hydrogen bonds to the side chain of Asp268 and the carbonyl group of the main chain ($-\text{C}=\text{O}$). The methyl group of L-alanine ($-\text{CH}_3$) is oriented towards the hydrophobic region bordered by Leu128. During the reaction, the water molecule (Wat) enters the reactive C in the substrate from a distance of 3.6 Å. The hydride transfer (H^-) distance to reactive C4 in NAD^+ as cofactor is 2.9 Å. In the lower part of the graphic, the carboxylate group of the pyruvate (green arrow) after catalysis binds to two hydrogen bonds Arg15 and the carbonyl group ($-\text{C}=\text{O}$) formed from the water molecule, and with two hydrogen bonds to Lys74 (2.0 Å) and His95 (1.8 Å). At the NADH ring, the distance of hydrogen from pyruvate is maintained at 2.9 Å.

(b) The oxidative deamination reaction of *TrAlaDH* with L-norleucine to α -ketocaproate. Oxygen is shown in red, nitrogen in blue, carbon in light brown and protons in white. The active site structures before and after the transition state are shown for key reaction stages for the hydride shift (hydride shown with red arrow) from L-norleucine to NAD^+ , and the transfer of a water molecule (Wat) to form α -ketocaproate. The interactions between the L-norleucine substrate (C_α shown with green arrow) and the α -ketocaproate product are shown in Ångströms. In the upper part of the graphic, the carboxylate group of L-norleucine ($-\text{COO}^-$) has three hydrogen bonds to Arg15 (2.2 Å), Lys74 (2.0 Å) and Asn299 (2.0 Å), and the distance from its amino group ($-\text{CH}_3^+$) to the Asp268 side chain and the carbonyl group of the main chain are 1.9 Å and 4.7 Å, respectively. The distance between the aliphatic chain of the substrate and Leu128 is 3.4 Å, the distance to His95 is 5.4 Å, and the distance of hydride transfer to the reactive C4 is 2.7 Å. In the lower part of the graphic, the binding of the α -ketocaproate (green arrow) carboxyl group after catalysis is shown. There are two hydrogen bonds with Arg15 (1.8 Å) and Lys74 (1.8 Å). The distance between the hydrophobic interaction of α -ketocaproate between the aliphatic side chain and Leu128 is 3.7 Å. The distance between the hydrogen at NADH to α -ketocaproate is 2.8 Å.

Discussion

A noteworthy finding of our study was the different temperature profiles associated with enzyme catalysis of *TrAlaDH*. The binding of substrate molecules can affect the thermal stability of enzymes [47]. Reductive deamination possibly occurs more at a higher temperature than amination. The optimal growth temperature for *T. roseum* is 70–75 °C [48], whereas *TrAlaDH* has an optimal catalytic temperature at 55–55°C. *TrAlaDH* is an intracellular enzyme, so it is possible that when the enzyme is purified, it is not as stable as when it is surrounded by other intracellular proteins. To date, optimum temperatures for alanine dehydrogenase enzymes have been reported in the range of 30–40 °C [49,50], 40–50 °C [32, 51] and 50–70 °C [15, 19,52]. The most extreme thermostability has been found for AlaDH from the extremophilic archaea *Archaeoglobus fulgidus*, which showed optimum activity at 82 °C for reductive amination of pyruvate [11].

Since the *T. roseum* microbe is found in alkaline hot springs [46], the optimum alkaline pH observed in our study fits well with natural conditions. The optimum pH for oxidative deamination reaction activity of AlaDHs from different sources has been reported as pH 6.4–7.4 [12], pH 9.5 [15,19], pH 10.0 [41], pH 10.0–11.0 [53] and pH 12 [12]. Mostly, these studied enzymes are alkaliphilic, with the exception of the archaeal *A. fulgidus* AlaDH, which has a neutral pH optimum [11]. Thus, the *TrAlaDH* optimum pH in oxidative deamination is similar to most other studied enzymes [12-15,19,53]. In contrast, the optimum pH for the reductive amination reaction of alanine dehydrogenase has been reported as pH 7.0–7.5 [52], pH 8 [12], pH 8.5 [42] and pH 9 [19]. This comparison indicates that the pH optimum of reductive amination typically occurs in less alkaline pH. The pH optimum of *TrAlaDH* for reductive amination is within the most alkaliphilic group. Moreover, *TrAlaDH* exhibited a wide pH activity range between pH 5 and 12, both in oxidative deamination and reductive amination reactions.

Various methods have been reported to produce L-alanine amino acid. Microbial production of L-alanine has gained much attention, but use has been limited since L-alanine is not produced with high yield [35]. Biosynthesis of L-Ala can be performed by glutamate dehydrogenase in two steps using α -ketoglutarate, ammonia and NADH as substrates. However, this multistep process is limited due to its high cost [36]. Immobilization of AlaDH cannot be used to produce L-Ala efficiently due to the loss of activity in the immobilized enzyme [6, 37]. Reductive amination of pyruvate was evaluated as the main function of AlaDH and this reaction synthesizes alanine for peptidoglycans *in vivo* [18,31,38-40]. This function could be adapted to synthesize L-Ala derivatives *in vitro*, since the reductive amination of keto acids by NAD⁺-dependent AlaDH has significant potential for the synthesis L-Ala and its derivatives. Although AlaDH exhibit wide substrate specificity in oxidative demination [18,41], they show selective activity towards pyruvate. Therefore, a number of AlaDH have been tested for pyruvate derivatives, such as 3-hydroxypyruvate and 2-oxoalate [19-22] in reductive deamination reactions. One well-known example is to produce L- β -fluoropalanine by utilizing AlaDH [43], although due to the large sequence diversity among AlaDHs, each AlaDH can exhibit variable reductive amination activity [9,16,24,33,42,44-46].

In this study, the reductive amination of the pyruvate derivatives that belong to the α -keto acid family were tested with *Tr*AlaDH. While activity was observed for α -ketobutyrate and α -ketoalate, which have four and five carbons, respectively, the six-carbon α -ketocaproate substrate was not aminated reductively at a measurable rate, even though L-norleucine, with the same carbon number, showed reactivity in oxidative demination (**Table 1**). Calculated kinetic parameters for AlaDHs from different organisms are summarized in **Table 4**.

Table 4. Kinetic parameter K_M and k_{cat} values of selected alanine dehydrogenases with L-alanine and pyruvate.

| Organism | L-Alanine | | Pyruvate | | Reference |
|--------------------------------|------------|------------------------|------------|------------------------|------------|
| | K_M (mM) | k_{cat} (s^{-1}) | K_M (mM) | k_{cat} (s^{-1}) | |
| <i>Bilophila wadsworthia</i> | 1.60 | - | 1.1 | - | [32] |
| <i>Vibrio proteolyticus</i> | 30.00 | - | 0.6 | - | [11] |
| <i>Thermus caldophilus</i> | 2.60 | - | 0.2 | - | [12] |
| <i>Arcohoeglobus fulgidus</i> | 0.70 | - | 0.2 | - | [13] |
| <i>Shewanella sp.</i> | 0.04 | 35 | - | - | [14] |
| <i>Phormidium lapideum</i> | 0.04 | 96 | - | - | [14] |
| <i>Thielaviopsis paradoxa</i> | 1.35 | - | 8.2 | - | [15] |
| <i>M. tuberculosis</i> | 4.30 | - | 2.8 | - | [33] |
| <i>Amycolatopsis sulphurea</i> | 2.03 | 13 | - | - | [9] |
| <i>M. tuberculosis</i> | 5.30 | 8 | - | - | [18] |
| <i>Streptomyces coelicolor</i> | - | 2 | - | 1.9 | [19] |
| <i>Archaeoglobus fulgidus</i> | - | - | 0.2 | 0.1 | [34] |
| <i>T. roseum</i> | 2.90 | 43 | 1.9 | 35.0 | This study |

Few studies have calculated the kinetic values for both oxidative deamination and reductive amination reactions for the enzyme from the same organism. The K_M values associated with L-AlaDH obtained from other organisms can vary considerably (0.035–30 mM) (**Table 4**), whereas the K_M value associated with TrAlaDH (2.7 mM) is within this range. While the best k_{cat} value has been reported for *Phormidium lapideum* ($95.5 s^{-1}$) [14], we calculated a value of $4.1 s^{-1}$ for TrAlaDH in this study. Few kinetic data have been reported for pyruvate and among these enzymes, TrAlaDH exhibited a greater k_{cat} value ($35 s^{-1}$). In our study, the K_M value for pyruvate with TrAlaDH is in the same range as reported for other L-AlaDHs (**Table 4**). The K_M values occurred across a wide range, and true comparisons may not be possible due to differing experimental conditions between studies, although we found a single study that reported kinetic values of *M. tuberculosis* AlaDH

(*MtAlaDH*) against L-alanine derivatives (**Table 5**). The oxidative deamination results of *TrAlaDH* with L-alanine derivatives were compared with that of a single study in literature [10] (**Table 4**). In that study, the *M. tuberculosis* enzyme seemed to react much better with L-norvaline than *TrAlaDH* in oxidative deamination. This indicates that there are significant differences between AlaDHs in their acceptance of various amino acids as a substrate.

Table 5. Kinetic efficiency values with L-alanine derivatives for two selected alanine dehydrogenases in oxidative deamination.

| | L- α -Aminobutyrate | L-Norvaline | L-Norleucine | Reference |
|------------------------|-----------------------------------|-----------------------------------|-----------------------------------|------------|
| Organism | k_{cat}/K_M ($M^{-1} s^{-1}$) | k_{cat}/K_M ($M^{-1} s^{-1}$) | k_{cat}/K_M ($M^{-1} s^{-1}$) | |
| <i>M. tuberculosis</i> | ----- | 0.40 ± 0.07 | <0.01 | [10] |
| <i>T. roseum</i> | 0.094 ± 0.0 | 0.0014 ± 0.0 | 0.0011 ± 0.0 | This study |

A number of microorganism-gene-derived AlaDH enzymes have been characterized to date (**Table 4**). Since both L-alanine and pyruvate exhibited similar K_M values, this would confirm that both bind similarly to the active site, although pyruvate exhibited a much greater k_{cat} value. One reason could be that pyruvate (with planar C_α) is able to find the reactive position much more easily. In our study, the K_M value for L-alanine (2.7 mM) was found to be similar (only 1.5-fold higher) to the average K_M values in the literature, with the exception of *Vibrio proteolyticus* AlaDH [9] (**Table 4**). In our study, pyruvate K_M and k_{cat} values were found to be 2.24- and 18.42-fold higher, respectively, compared to the literature (**Table 4**). Catalytic reaction studies with the L-alanine derivatives, such as L- α -aminobutyrate, L-norvaline and L-norleucine, are extremely limited (**Table 5**). Similarly, there is limited information about derivatives undergoing reductive deamination [19-22]. While α -ketocaproate was not identified in the enzyme activity studies in our study, a new understanding was observed for α -ketobutyrate and α -ketovalerate (**Table 1**).

The AlaDH enzymes could be used to synthesize single isomeric unnatural amino acid derivatives from pyruvate derivatives [2,3]. This would require a more effective reductive reaction with the pyruvate derivatives. Therefore, it is necessary to acquire a deeper structure-based understanding of the catalytic mechanism and interactions with large substrates. *TrAlaDH* is a NAD-dependent dehydrogenase that catalyzes a multi-step hydride transfer reaction from alanine to pyruvate and *vice versa*. Reactions are redox reactions of two substrates, L-alanine with NAD⁺ and pyruvate with NADH (**Figure 1**). According to our results, the positioning of various L-alanine derivatives with NAD(H) and thus their potential to be substrates in the reductive reaction can be analyzed. Reactions measured with L-alanine derivatives show that catalysis activity also exists with larger molecules than L-alanine, although the effectiveness of catalysis decreased greatly according to their much higher K_M values.

The differences in the kinetic values between the amination and deamination reactions can be explained by the presence or absence of the amino group and the presence of a longer aliphatic side chain. From the K_M values, it can be seen that the presence of the amino group at C_α affects the binding of the substrate considerably, apparently even more significantly than aliphatic group size, once the molecule is larger than L-alanine (**Table 1**). The influence of different structures can be seen in both the k_{cat} and k_{cat}/K_M values. Since pyruvate has a greater k_{cat}/K_M ratio than L-alanine, then the planar molecule is more favorable for reductive amination, even though both L-alanine and pyruvate have a similar affinity to the active site. The larger size of the aliphatic side chain among pyruvate, α -ketoglutarate and α -ketovalerate does not unduly affect K_M but does impair the k_{cat} value.

The values shown in **Table 2** indicate that the enzyme has promising reaction rates with several substrates. The calculations concern conversion rates in low substrate concentrations. Industrially relevant high substrate concentrations and cofactor strategy

require further studies. Earlier studies also showed that *Corynebacterium gelatinosium*, *Arthrobacter oxydans*, *Brevibacterium lactofermentum*, *Clostridium sp.* and *Pyrococcus furiosus*, produced L-alanine with a maximum conversion rate of 10 to 60% [54]. Also other substrates have been studied [55].

The crystal structure of *M. tuberculosis* AlaDH (2voj.pdb) indicates that it contains a water molecule near pyruvate (distance 3.6 Å). The existence of a water molecule indicates possible free space for a side chain larger than the methyl group, and for the NH_4^+ group to settle at the active site. The molecular model of *T. roseum* AlaDH and the crystal structure of *M. tuberculosis* AlaDH suggest that the binding site amino acids Tyr93, Leu128 and Met131 form a clear hydrophobic environment (Fig. 6) and that substrate aliphatic side chains can orient toward it. The hydrophobic region that binds the aliphatic groups also controls the position of the substrates for the catalysis. Both structures have a large flexible loop area (amino acids 264–286), and especially, four amino acids 267–270 may have effect on the access of the substrate to the active site and the position close to the NADH in it. Planar keto form substrates lack a NH_3 group and exhibit a different configuration at C_α (green arrows in Figure 6 show C_α position, at which big structural differences exist between pyruvate and L-alanine) and therefore, have more room to bind with a salt bridge to arginine and with a hydrogen bond to lysine. This is favorable for reductive amination because the positive charge of lysine can amplify the electrophilicity of the carbon of the carboxyl group as it exhibits attraction to the double bond electrons. Therefore, the reaction rate with pyruvate is much higher than with L-alanine as substrate.

Cations that may be present in the reaction environment could affect the transfer of electrons in the reaction and they may cause repulsion with NH_4^+ and with NAD^+ molecules. The cations Na^+ and K^+ may act as the oxidative deamination inhibitor, and in the reductive amination Li^+ and K^+ may accelerate it. Mn^{2+} and W^{6+} can also act as accelerators in the

oxidative reaction, while iron seems to strongly inhibit the reaction. In the reductive amination, inhibiting cations are Mg^{2+} , Zn^{2+} and Fe^{3+} (**Table 3**). This might possibly indicate that a repulsion force prevents the departure of NH_4^+ in the deamination reaction, whereas the effect is positive in the amination reaction.

Derivatives of both pyruvate and L-alanine are acceptable as substrates. However, with a large side chain they may have challenges to bind correctly in respect to reaction with NADH, although according to the modeled structures they can fit into the active site. Highly conservative amino acids such as Arg15, Lys74, His95 with hydrogen bonds to the substrate or NADH are likely to be critical for the enzyme catalysis. On the other hand, the modeling with larger substrates shows that there is space for the aliphatic part of different substrates to fit into the area between Tyr93, His95, Leu128, Met131 and the nicotinamide ring of cofactor NADH. However, the slow catalysis rates indicate that the positioning of the bigger substrates becomes restricted in non-optimal way.

Conclusions

In this study, we analyzed the biochemical behavior of heterologously expressed and purified *TrAlaDH* in reductive amination and oxidative deamination reactions. The reaction mechanism is based on hydride transfer, proton transfer and oxidative amino-to-ketone interconversion. Previous structural L-alanine dehydrogenase studies [26,56,57] and molecular modeling of *TrAlaDH* was used to generate an understanding of the enzyme reaction with L-alanine and pyruvate derivatives. The *TrAlaDH* enzyme exhibited significant potential to recognize selected various keto acids and L-alanine derivatives. The biochemical studies and active site analysis showed that larger derivatives of L-alanine and pyruvate were accepted as substrates, and they have space to bind onto the active site. These results support the possibility to develop new biocatalytic tools (by protein engineering) from these enzymes

and utilize them in biocatalysis to synthesize non-natural amino acids [18]. Further studies are needed to improve the conditions to obtain soluble enzymes while performing scale-up studies and this would also provide how the chiral differences of the L-alanine derivatives (compared to corresponding keto acids) affect the reaction efficiency with *TrAlaDH*, and how the reaction efficiency could be improved by active site mutations.

Declaration of interests

The authors declare that they have no known competing financial interests or personal relationships that could have appeared to influence the work reported in this paper.

The authors declare the following financial interests/personal relationships which may be considered as potential competing interests:

Baris Binay reports financial support was provided by Turkish Academic Network and Information Centre.

Acknowledgement:

This work was supported partially by TUBITAK (Project number: 120Z501). We thank Mr. Jouni Oljakka (Master of Science in Mathematics) for the statistical analysis of the data.

Conflict of interest:

The authors declare no conflicts of interest.

References:

- [1] Narancic T, Almahboub SA, O'Connor KE. Unnatural amino acids: production and biotechnological potential. *World Journal of Microbiology and Biotechnology*. 2019; 35(4), 1-11.
- [2] Polis B, Srikanth KD, Gurevich V, et al. L-Norvaline, a new therapeutic agent against Alzheimer's disease. *Neural regeneration research*. 2019; 14(9), 1562.
- [3] Thomas AJ, Ismail R, Taylor-Swanson L, et al. Effects of isoflavones and amino acid therapies for hot flashes and co-occurring symptoms during the menopausal transition and early postmenopause: a systematic review. *Maturitas*. 2014; 78(4), 263-276.
- [4] Perdih A, Dolenc MS. Recent advances in the synthesis of unnatural α -amino acids. *Current Organic Chemistry*. 2007; 11(9), 801-832.
- [5] Ferraris D, Young B, Cox C, et al. Catalytic, enantioselective alkylation of α -imino esters: The synthesis of nonnatural α -amino acid derivatives. *Journal of the American Chemical Society*. 2002; 124(1), 67-77.

- [6] Dave UC, Kadeppagari RK. Alanine dehydrogenase and its applications—A review. In *Critical Reviews in Biotechnology*. 2019; 39, 648–664.
- [7] Zhou J, Wang Y, Chen J, et al. Rational Engineering of *Bacillus cereus* Leucine Dehydrogenase Towards α -keto Acid Reduction for Improving Unnatural Amino Acid Production. *Biotechnology Journal*. 2019; 14(3), 1800253.
- [8] Ashida H, Sawa Y, Yoshimura T. Enzymatic determination of D-alanine with L-alanine dehydrogenase and alanine racemase. *Bioscience, Biotechnology, and Biochemistry*. 2021; 85(11), 2221-2223.
- [9] Aktaş F. Heterologous Expression and Partial Characterization of a New Alanine Dehydrogenase from *Amycolatopsis sulphurea*. *The Protein Journal*. 2021; 40(3), 342-347.
- [10] Chen G, Tan Z, Liu Y, et al. Function and characterization of an alanine dehydrogenase homolog from *Nocardia seriolae*. *Frontiers in veterinary science*. 2021; 8.
- [11] Kato SI, Ohshima T, Galkin A, et al. Purification and characterization of alanine dehydrogenase from a marine bacterium, *Vibrio proteolyticus*. *Journal of Molecular Catalysis B: Enzymatic*. 2003; 23(2–6), 373–378.
- [12] Bae JD, Cho YJ, Kim DI, et al. Purification and biochemical characterization of recombinant alanine dehydrogenase from *Thermus caldophilus* GK24. *Journal of Microbiology and Biotechnology*. 2003; 13(4), 628–631.
- [13] Schröder I, Vadas A, Johnson E, et al. A novel archaeal alanine dehydrogenase homologous to ornithine cyclodeaminase and μ -crystallin. *Journal of Bacteriology*. 2004; 186(22), 7680–7689.
- [14] Ashida H, Galkin A, Kulakova L, et al. Conversion of cofactor specificities of alanine dehydrogenases by site-directed mutagenesis. *Journal of Molecular Catalysis B: Enzymatic*. 2004; 30(3–4), 173–176.
- [15] Al-Onazi M, Al-Dahain S, El-Ansary A, et al. Isolation and characterization of *Thielaviopsis paradoxa* L-alanine dehydrogenase. *Asian Journal of Applied Sciences*. 2011; 4(7), 702–711.
- [16] Gallagher TG, Monbouquette HG, Schröder I, et al. Structure of alanine dehydrogenase from *Archaeoglobus*: Active site analysis and relation to bacterial cyclodeaminases and mammalian μ crystallin. *J. Mol. Biol.* 2004; 342, 119–130.
- [17] Hyun CG, Kim SS, Lee IH, et al. Alteration of substrate specificity of valine dehydrogenase from *Streptomyces albus*. *Int. J. Gen. Mol. Microbiol.* 2000; 78, 237–242.
- [18] Fernandes P, Aldeborgh H, Carlucci L, et al. Alteration of substrate specificity of alanine dehydrogenase. *Protein Engineering, Design and Selection*. 2015; 28(2), 29–35.
- [19] Wieren AV, Cook R, Majumdar S. Characterization of alanine dehydrogenase and its effect on *Streptomyces coelicolor* A3(2) development in liquid culture. *J. Mol. Microbiol. Biotechnol.* 1–9. 2019;29(1-6):57-65.
- [20] Ohashima T, Soda K. Purification and properties of alanine dehydrogenase from *Bacillus sphaericus*. *Eur J Biochem.* 1979; 100:29–39.
- [21] Bellion E, Tan F. An NAD β -dependent alanine dehydrogenase from a methylotrophic bacterium. *Biochem J.* 1987; 244:565–570.
- [22] Aharonowitz Y, Friedrich CG. Alanine dehydrogenase of the beta-lactam antibiotic producer *Streptomyces clavuligerus*. *Arch Microbiol.* 1980; 125:137–142.
- [23] Studier FW. Protein production by auto-induction in high density shaking cultures. *Protein Expr Purif.* 2005; 41, 207–234.
- [24] Chang A, Jeske L, Ulbrich S, et al. BRENDA, the ELIXIR core data resource in 2021: new developments and updates. *Nucleic Acids Research*. 2021; 49(D1), D498-D508.
- [25] Palmer T, Bonner P. *Enzymes, Biochemistry, Biotechnology, Clinical Chemistry*. 2007; Elsevier

- [26] Waterhouse A, Bertoni M, Bienert S, et al. SWISS-MODEL: Homology modelling of protein structures and complexes. *Nucleic Acids Research*. 2018; 46(W1), W296–W303.
- [27] Tripathi SM, Ramachandran R. Crystal structures of the Mycobacterium tuberculosis secretory antigen alanine dehydrogenase (Rv2780) in apo and ternary complex forms captures “open” and “closed” enzyme conformations. *Proteins: Structure, Function and Genetics*. 2008;72(3), 1089–1095.
- [28] Krieger E, Joo K, Lee J, et al. Improving physical realism, stereochemistry, and side-chain accuracy in homology modeling: Four approaches that performed well in CASP8 Proteins. 2009;77 Suppl 9:114-22.
- [29] Pettersen EF, Goddard TD, Huang CC, et al. UCSF Chimera--a visualization system for exploratory research and analysis. *J Comput Chem*. 2004;25(13):1605-12.
- [30] Bulut H, Valjakka J, Yuksel B, Yilmazer B, Turunen O, Binay B. Effect of metal ions on the activity of ten NAD-dependent formate dehydrogenases. *The Protein Journal*. 2020; 39, 519-530.
- [31] Hu X, Bai Y, Fan TP, Zheng X, Cai Y. A novel type alanine dehydrogenase from *Helicobacter aurati*: Molecular characterization and application. *International Journal of Biological Macromolecules*. 2020; 161, 636-642.
- [32] Laue H, Cook AM. Purification, properties and primary structure of alanine dehydrogenase involved in taurine metabolism in the anaerobe *Bifidobacterium wadsworthia*. *Archives of Microbiology*. 2000; 174(3), 162–167.
- [33] Giffin MM, Modesti L, Raab RW, et al. *Ald* of mycobacterium tuberculosis encodes both the alanine dehydrogenase and the putative glycine dehydrogenase. *Journal of Bacteriology*. 2012;194(5), 1045–1054.
- [34] Gmelch TJ, Sperl JM, Sieber V. Optimization of a reduced enzymatic reaction cascade for the production of L-alanine. *Scientific Reports*. 2019; 9(1), 1–9.
- [35] Liu P, Xu H, Zhang X. Metabolic engineering of microorganisms for L-alanine production. *Journal of Industrial Microbiology and Biotechnology*. 2022; 49(2), 57.
- [36] Mathews CK, Van Holde KE, Ahern KG. *Biochemistry*. 2000. 3rd ed. San Francisco, Calif. : Benjamin Cummings.
- [37] Ren, Li C, Jiao X, et al. Recent progress in multienzymes co-immobilization and multienzyme system applications. *Chemical Engineering Journal*. 2019; 373, 1254-1278.
- [38] Akita H, Hayashi J, Sakubara H, et al. Artificial Thermostable D-Amino Acid Dehydrogenase: Creation and Application. *Frontiers in Microbiology*. 2018;9,1760.
- [39] Giffin MM, Shi L, Gennaro ML, et al. Role of Alanine dehydrogenase of *Mycobacterium tuberculosis* during recovery from hypoxic nonreplicating persistence. *PLoS One*. 2016;11:1–18.
- [40] Parker MF, Luu JM, Schulte B, et al. Sensing living bacteria in vivo using d-alanine-derived ¹¹C radiotracers. *ACS central science*. 2020; 6(2), 155-165.
- [41] Hu., Bai Y, Fan TP, et al. A novel type alanine dehydrogenase from *Helicobacter aurati*: Molecular characterization and application. *International Journal of Biological Macromolecules*. 2020;161, 636-642.
- [42] Dave UC, Kadeppagari RK. Purification and characterization of Alanine dehydrogenase from *Streptomyces anulatus* for its application as a bioreceptor in biosensor. *Process Biochemistry*. 2018; 68, 73–82.
- [43] Ohshima T, Wandrey C, Conrad D. Continuous production of 3-fluoro-L-alanine with alanine dehydrogenase. *Biotechnology and bioengineering*. 1989; 34(3), 394-397.
- [44] Jeong JA, Oh JI. Alanine dehydrogenases in mycobacteria. *Journal of Microbiology*. 2019; 57(2), 81-92.

- [45] Roura Padrosa D, Nisar Z, Paradisi F. Efficient amino donor recycling in amination reactions: development of a new alanine dehydrogenase in continuous flow and dialysis membrane reactors. *Catalysts*. 2021; 11(4), 520.
- [46] Li R, Chen Y, Du K, et al. Peptide Bond Formation Between the Heterosubunits of ω -Transaminase, Alanine Dehydrogenase, and Formate Dehydrogenase Through Subunit Splicing Promoted by Heterodimerization of Leucine Zipper Motifs. *Frontiers in bioengineering and biotechnology*. 2020; 8, 686.
- [47] Anbarasan, S., Jänis, J., Paloheimo, M. Laitaoja, M. Vuolanto, M., Karimäki, J., Vainiotalo P, Leisola M, Turunen O. Effect of pH, glycosylation and additional domains on the thermostability of family 10 xylanase of *Thermopolyspora flexuosa*. *Appl. Environ. Microbiol.* 2020;76: 356-360.
- [48] Wu D, Raymond J, Wu M, et al. Complete genome sequence of the aerobic CO-oxidizing thermophile *Thermomicrobium roseum*. *PLoS ONE*. 2009; 4(1).
- [49] Ye W, Huo G, Chen J, et al. Heterologous expression of the *Bacillus subtilis* (natto) alanine dehydrogenase in *Escherichia coli* and *Lactococcus lactis*. *Microbiological Research*. 2010;165(4), 268–275.
- [50] Nakane K, Suye SI, Ueno T, et al. Coimmobilization of malic enzyme and alanine dehydrogenase on organic-inorganic hybrid gel fibers and the production of L-alanine from malic acid using the fibers with coenzyme regeneration. *J. Appl. Polym. Sci.* 2010;116, 5.
- [51] Irwin JA, Lynch SV, Coughlan S, et al. Alanine dehydrogenase from the psychrophilic bacterium strain PA-43: Overexpression, molecular characterization, and sequence analysis. *Extremophiles*. 2003;7(2), 135–143.
- [52] Heydari M, Ohshima T, Nunoura-Kominato N, et al. Highly Stable L-Lysine 6-Dehydrogenase from the Thermophile *Geobacillus stearothermophilus* Isolated from a Japanese Hot Spring: Characterization, Gene Cloning and Sequencing, and Expression. *Applied and Environmental Microbiology*. 2004;70(2), 937–942.
- [53] Hutter B, Singh M. Properties of the 40 kDa antigen of *Mycobacterium tuberculosis*, a functional L-alanine dehydrogenase. *Biochemical Journal*. 1999; 343(3), 669–672.
- [54] Hols P, Kleerebezem M, Kuipers OP, et al. Process for the production of alanine by recombinant microorganisms. Washington, DC: U.S. Patent and Trademark Office. 2003.
- [55] Marchini V, Benítez-Mateos A. I, Hutter L, et al. Fusion of Formate Dehydrogenase and Alanine Dehydrogenase as an Amino Donor Regenerating System Coupled to Transaminases. *ChemBioChem*. 2022; 23(21), e202200428.
- [56] Ågren D, Stehr M, Berthold CL, et al. Three-Dimensional Structures of Apo- and Holo-l-Alanine Dehydrogenase from *Mycobacterium tuberculosis* Reveal Conformational Changes upon Coenzyme Binding. *Journal of Molecular Biology*. 2008;377(4), 1161–1173.
- [57] Aslan AS, Valjakka J, Ruupunen J, et al. *Chaetomium thermophilum* formate dehydrogenase has high activity in the reduction of hydrogen carbonate (HCO_3^-) to formate. *Protein Engineering, Design & Selection: PEDS*. 2017; 30(1), 47–55.

Highlights

- *TrAlaDH* was heterologously expressed in *E. coli* cells.
- *TrAlaDH* was characterized kinetically with non-natural substrates.
- The enzyme was more efficient in amination than deamination reactions.
- Active site modeling revealed the possible reasons for substrate preferences.